Tema 6

Nucleosíntesis estelar de núcleos ligeros (A<60)

Asignatura de Astrofísica Nuclear

Curso académico 2009/2010

Universidad de Santiago de Compostela

Hydrostatic hydrogen burning

1.1 Stellar scenario

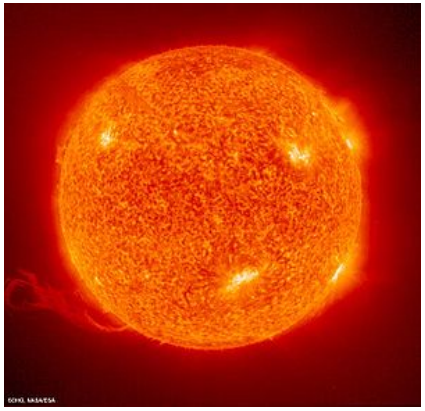

Thermonuclear reactions supplies the power that is irradiated from the stellar surface and provide the necessary internal pressure that prevents stars from collapsing gravitationally.

Reactions involving the smallest Coulomb barrier will proceed most rapidly and will account for most of the energy generation. Consequently, we expect nuclear reactions involving hydrogen and helium to be the main energy sources in most stars.

Hydrogen burning releases far more energy per unit fuel consumed compared to any other reaction. Thus, a star will consume its hydrogen fuel much more slowly than other fuel in order to balance both gravity and the energy radiated from its surface. Thus, as many as about 90% of the stars we observe belong to the main sequence where hydrogen is burnt.

Hydrogen burning takes place in the core of main sequence stars at typical temperatures of *T~8-55 MK* or in the outer shells of AGB stars at temperatures of *T=45-100 MK*.

Hydrostatic hydrogen burning

1.2 pp chains

The fusion of four ^{1}H nuclei to produce one ^{4}He nucleus is called *hydrogen burning*. Independently on the particular thermonuclear reactions involved the process always releases two positrons, two neutrinos and 24.7 MeV in form of gamma ratiation.

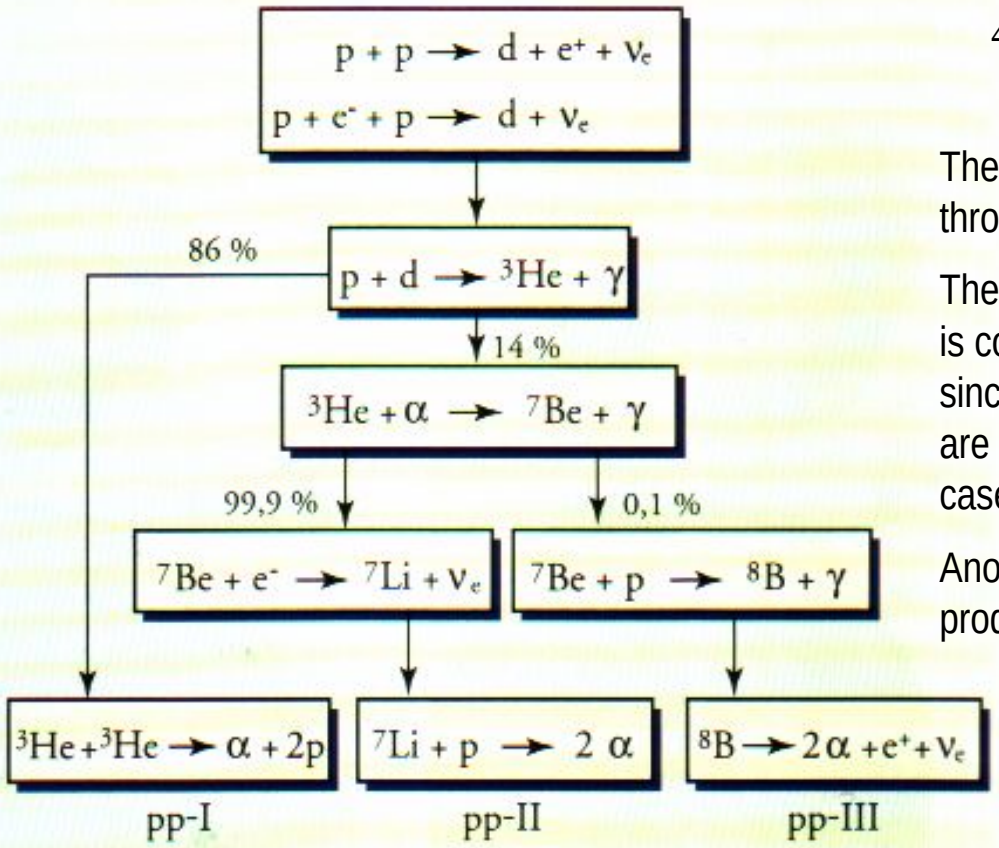

$$4\,p \rightarrow {}^{4}He + 2e^{+} + 2\,\nu_{e} + 24.7\ \mathrm{MeV}$$

The transformation of 1H into 4He can proceed in stars through three different reaction chains, called pp-cycles.

The first reaction leading to the production of deuterium is common to the three cycles. This is an special case since unlike almost all other stellar fusion reactions which are governed by the strong and Coulomb forces, in this case the weak force acts converting a proton into a neutron.

Another particularity of these reactions chains is neutrino production.

Hydrostatic hydrogen burning

1.3 Solar neutrino puzzle

Reactions involved in the pp-cycle produced electron-neutrinos with different energy ranges. Until recently The neutrino fluxes detected on Earth experiments did not agree with the Solar model stimates.

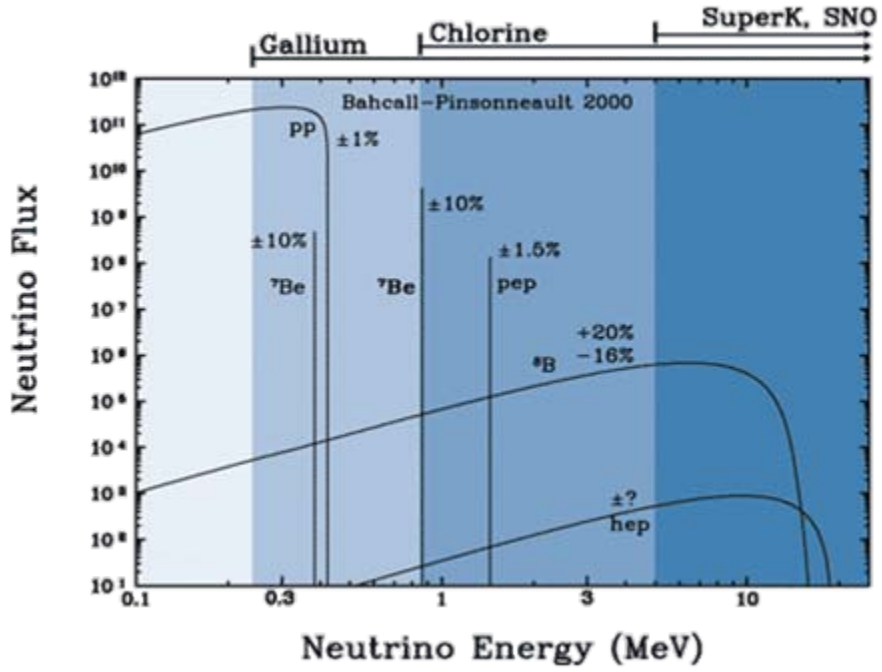

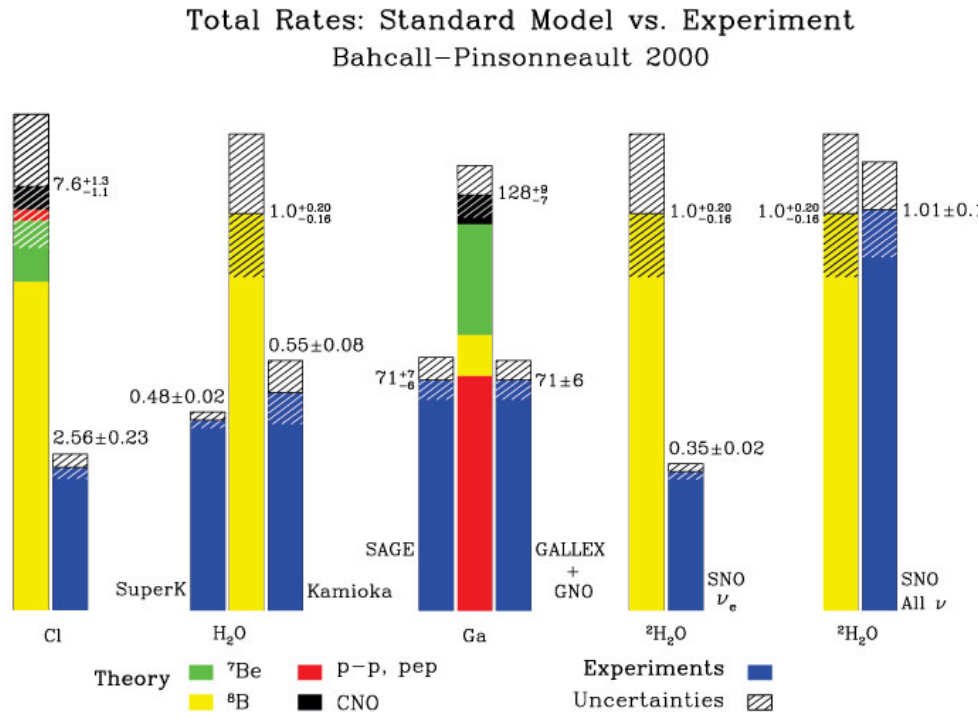

Few years ago, the SNO experiment in Canada provided an answer to the solar neutrino puzzle, neutrino oscillation explains the deficit of solar neutrinos observed on Earth.

Hydrostatic hydrogen burning

1.4 CNO cycles

Most of the stars do not only contain hydrogen and helium but also some small concentrations of heavier Nuclei like C, N , O and F. We know these heavier nuclei also participate in the hydrogen burning process as catalysts. We identify four reactions chains where hydrogen is converted into helium under the presence of C, N or O. These reaction chains are known as *CNO cycles*. The result of these cycles is exactly the same as the one obtain for the pp cycles:

$$4\,p \rightarrow {}^{4}He + 2e^{+} + 2\nu_e + 24.7\ \mathrm{MeV}$$

In these cycles C,N, O and F nuclei act only as catalysts, in the sense that the total abundance of the heavy nuclei is not altered while only hydrogen is consumed. The energy generation rate depends on the abundance of the catalysts nuclei and the time it takes to complete the cycle.

At low stellar temperatures (T<55 MK) b+ decays of unstable nuclei in the CNO mass range proceed much faster than proton capture. Thus, reactions involving unstable nuclei are unimportant. At higher temperatures, hot CNO cycle, the cycles change substantially.

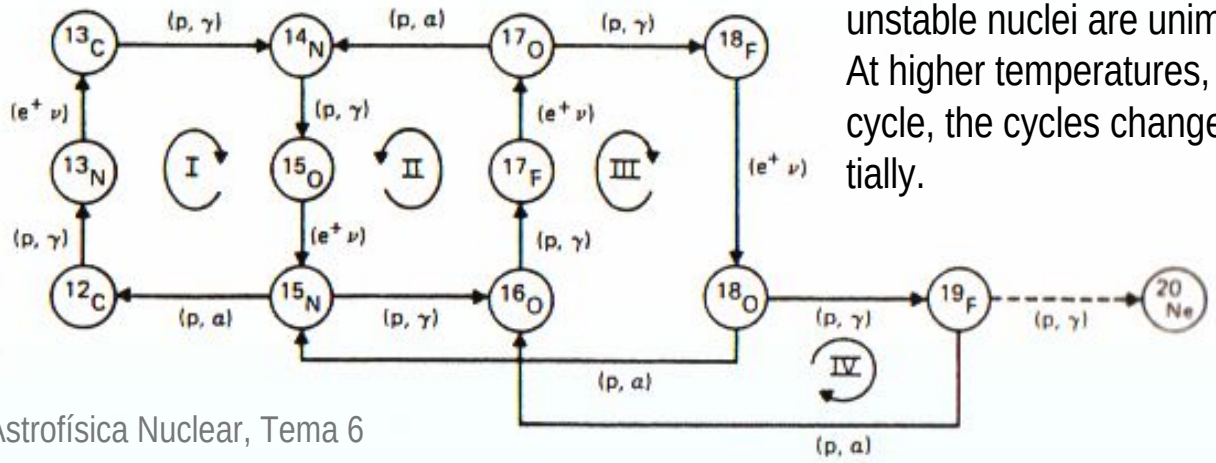

CNO1 cycle

$$^{12}C + p \rightarrow {}^{13}N + \gamma$$

$$^{13}N \rightarrow {}^{13}C + e^{+} + \nu_e$$

$$^{13}C + p \rightarrow {}^{14}N + \gamma$$

$$^{14}N + p \rightarrow {}^{16}O + \gamma$$

$$^{15}O \rightarrow {}^{15}N + e^{+} + \nu_e$$

$$^{15}N + p \rightarrow {}^{12}C + {}^{4}He$$

Hydrostatic hydrogen burning

1.5 Hydrostatic hydrogen burning beyond the CNO mass region

Nuclei heavier than F can also contribute to the hydrostatic hydrogen burning. However, the fact that the reaction rate for $^{19}F(p,\gamma)^{20}Ne$ is orders of magnitude smaller compared to the competing $^{19}F(p,\alpha)^{16}O$ reaction requires pre-existing seed nuclei with masses A>20.

As in the previous cycles, protons proton-induced reactions involving unstable nuclei play no significant role, except in the case of ^{26}Al having a half life of $T_{1/2}=7.2\ 10^5$ y.

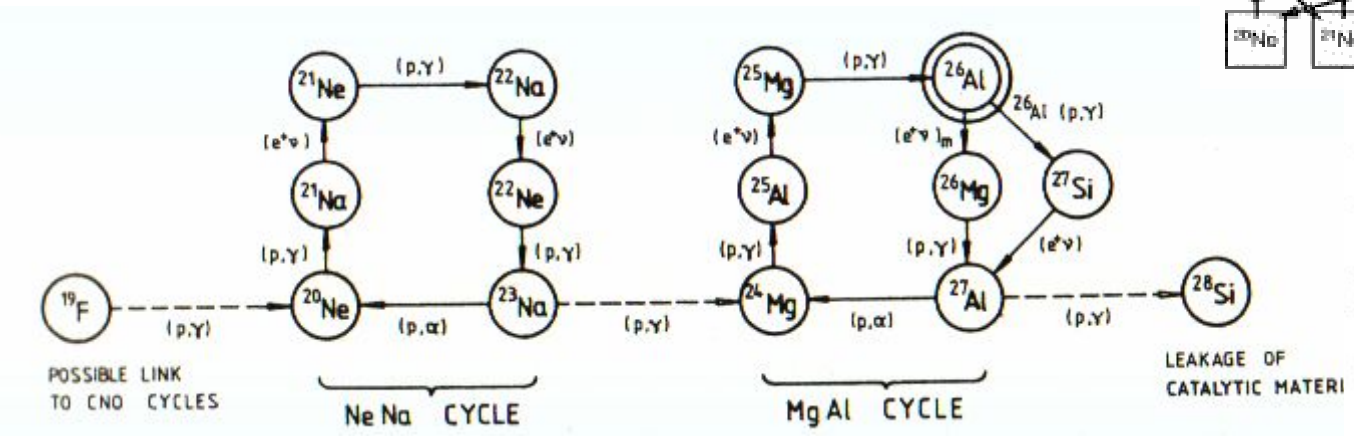

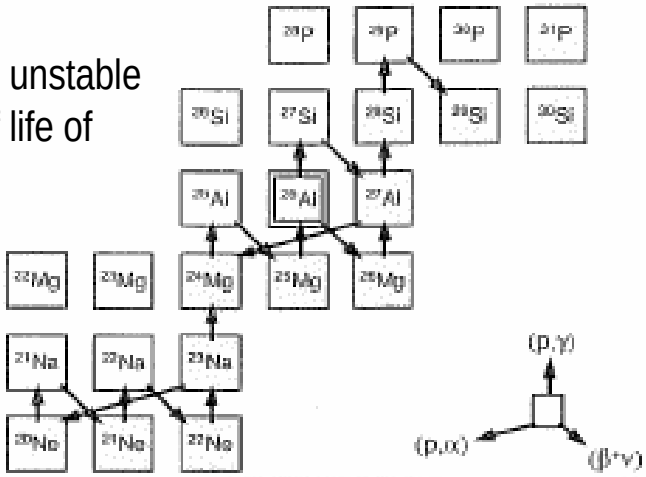

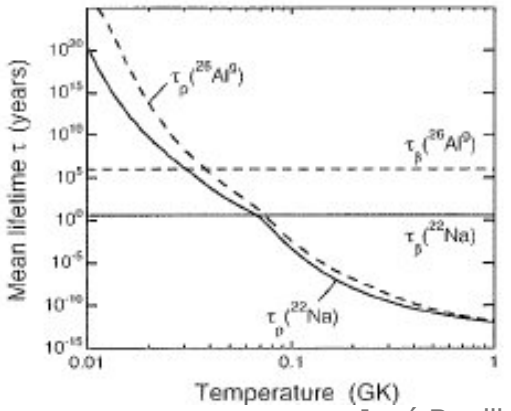

Hydrostatic hydrogen burning

1.5 Hydrostatic hydrogen burning beyond the CNO mass region

If a significant fraction of CNO nuclei is present in the stellar gas, then the CNO cycles will generate most Of the energy above a certain value of the temperature.

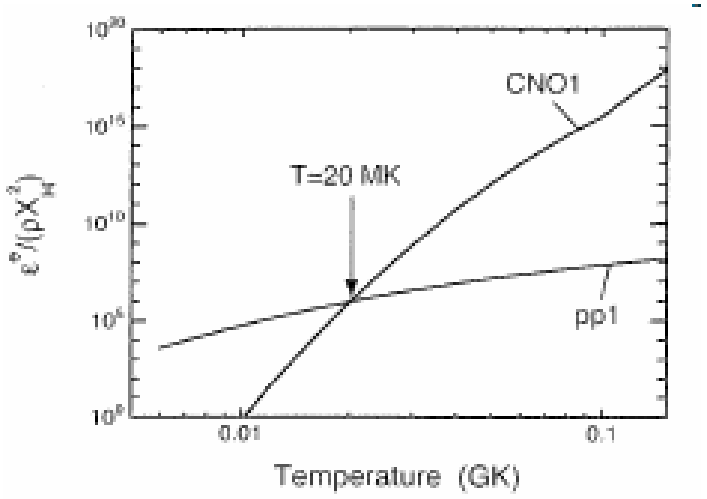

Hydrostatic hydrogen burning

1.6 Experimental investigation of key reactions

The Gamow window for the pp and CNO cycles in hidrostatic equilibrium correspond to CM energies below 200 keV. In this energy range cross sections are very small and the experimental investigation is limited by statistics: very long experiments with low background conditions.

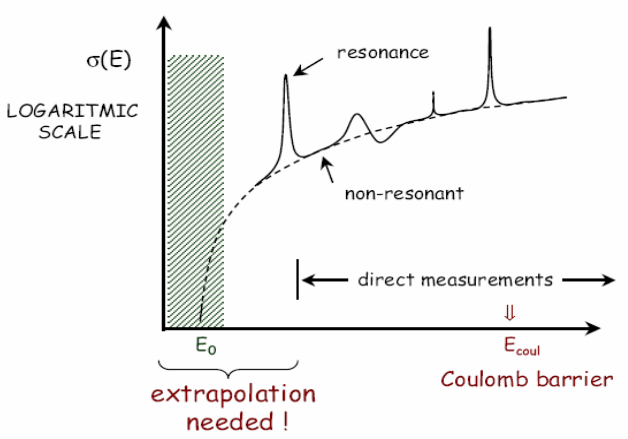

LUNA experiment at Gran Sasso Underground laboratory

LUNA2 Van der Graaf accelerator

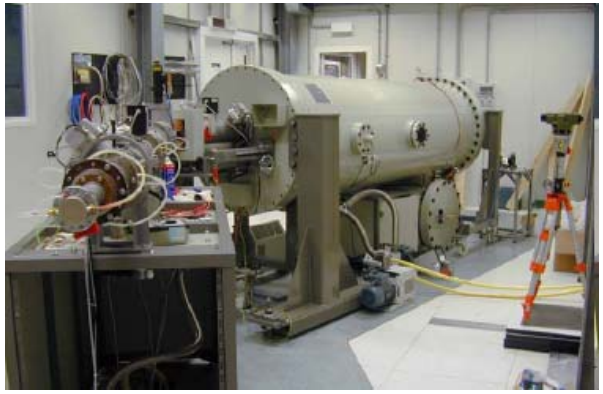

Hydrostatic hydrogen burning

1.6 Experimental investigation of key reactions

Experimental program at LUNA, Gran Sasso

- LUNA1 (1991, 50 kV) cp-p cycle: $^{3}He(^{3}He,2p)^{4}He$, $^{2}H(p,\gamma)^{3}He$ and $^{3}He(\alpha,\gamma)^{7}Be$
- LUNA2 (2000, 400 kV) CNO cycle: $^{14}N(p,\gamma)^{15}O$
- LUNA2 (2006, 400 kV) proposed measurements: $^{25}Mg(p,\gamma)^{26}Al$, $^{15}N(p,\gamma)^{16}O$, $^{2}H(\alpha,\gamma)^{6}Li$, $^{17}O(p,\gamma)^{18}F$, $^{18}O(p,\gamma)^{19}F$, $^{22}Ne(p,\gamma)^{23}Na$, $^{23}Na(p,\gamma)^{24}Mg$
- LUNA3 (????, 3MV) proposed experiments: $^{12}C(\alpha,\gamma)^{16}O$, $^{13}C(\alpha,n)^{16}O$, $^{22}Ne(\alpha,n)^{25}Mg$

Other initiatives in Europe:

- Canfranc Undergrund Laboratory, Spain
- Boulby, UK
- Slanic-Prahova, Romania

Initiatives in USA

- DUSEL, experiment

$$^{3}He + ^{4}He = ^{7}Be + \gamma$$

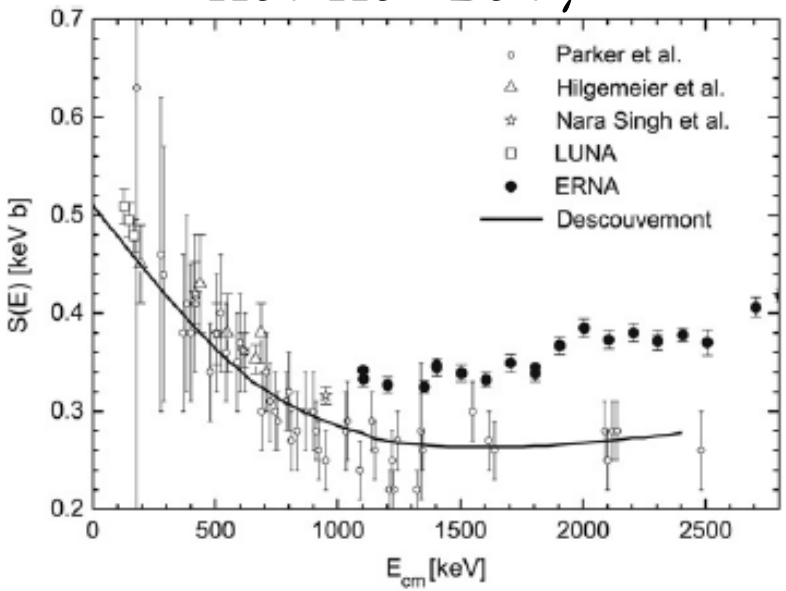

Hydrostatic hydrogen burning

1.6 Experimental investigation of key reactions

Canfranc Underground Laboratory

Experimental program:
- dark matter search
- double beta decay
- nucler astrophysics

Hot hydrogen burning

2.1 Stellar scenario

Hot hydrogen burning takes place at stellar temperatures between 0.1 and 0.4 GK. Those temperatures are reached in two scenarios:

✓ massive *Aymptotic Giant Branch* (AGB) stars ($M>4M_O$)

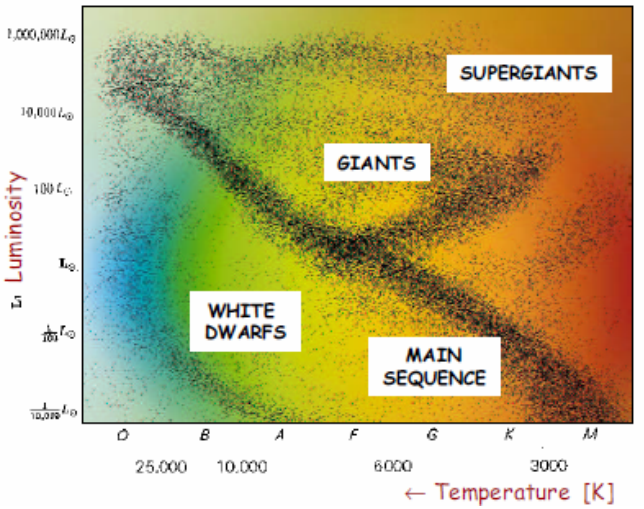

✓ *Novae phenomenon*

binary system made of:

white dwarf
(dead star mainky CO or ONe)

+

Red giant
H-shell burning and He burning

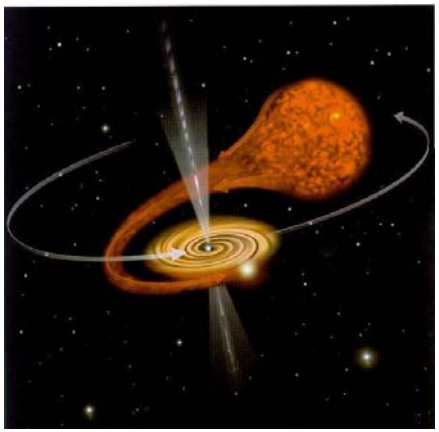

The main differences between hidrostatic and hot burning are:

- radioactive nuclei can induce proton-capture reactions.
- temperatures and densities in an explosive event change dramatically with time.

Hot hydrogen burning

2.2 Hot CNO cycle

Cold CNO

$T_9 < 0.08$ GK

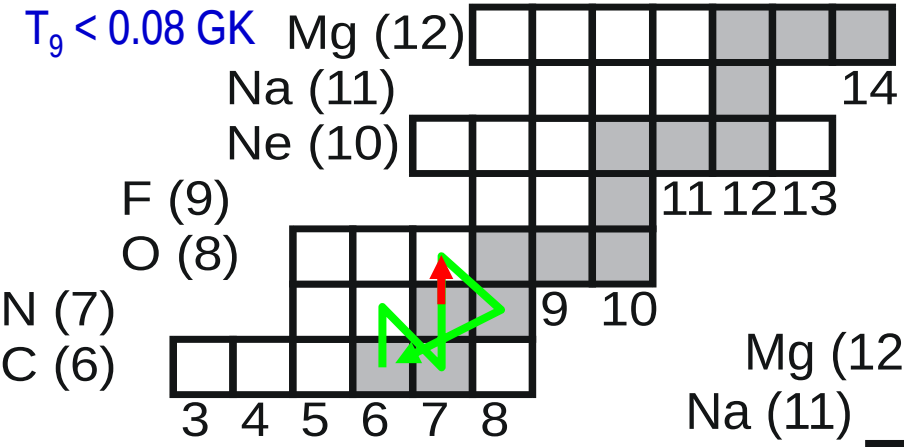

Proton capture reaction rates increase with temperature compiting then with beta decay and modifying the CNO cycles. At even higher temperatures α capture reactions compete with proton capture and β^+ decay.

Hot CNO

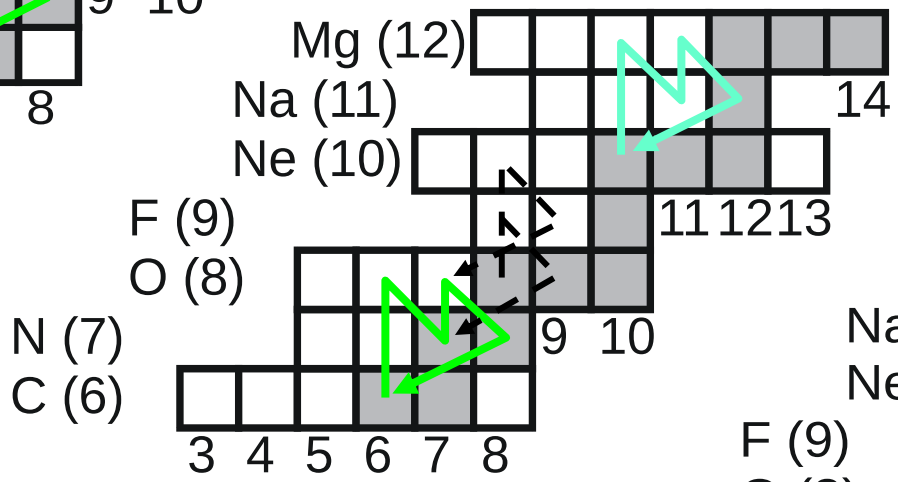

$T_9 \sim 0.08$-0.1 GK

Hot CNO + α burning

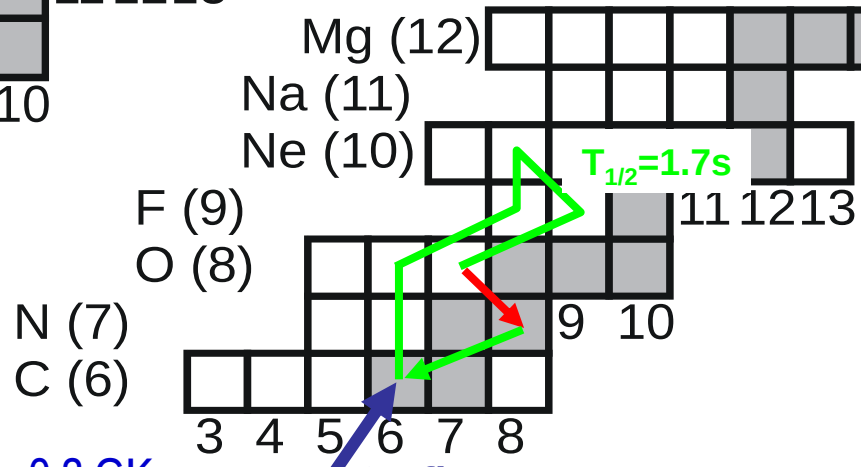

$T_9 \sim 0.3$ GK

Hot hydrogen burning

2.2 Hot CNO cycle

One can identify three hot CNO cycles

Hot CNO1	Hot CNO2	Hot CNO3
$^{12}C(p,\gamma)^{13}N$	$^{15}O(\beta^+\nu)^{15}N$	$^{15}O(\beta^+\nu)^{15}N$
$^{13}N(p,\gamma)^{14}O$	$^{15}N(p,\gamma)^{16}O$	$^{15}N(p,\gamma)^{16}O$
$^{14}O(\beta^+\nu)^{14}N$	$^{16}O(p,\gamma)^{17}F$	$^{16}O(p,\gamma)^{17}F$
$^{14}N(p,\gamma)^{15}O$	$^{17}F(\beta^+\nu)^{17}O$	$^{17}F(p,\gamma)^{18}Ne$
$^{15}O(\beta^+\nu)^{15}N$	$^{17}O(p,\gamma)^{18}F$	$^{18}Ne(\beta^+\nu)^{18}F$
$^{15}N(p,\alpha)^{12}C$	$^{18}F(p,\alpha)^{15}O$	$^{18}F(p,\alpha)^{15}O$

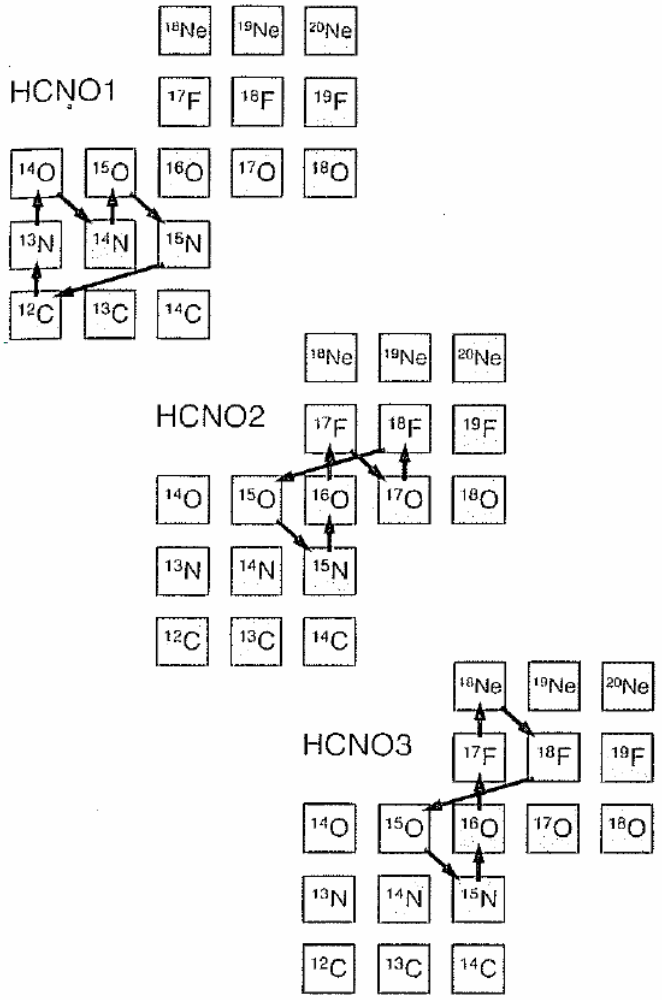

Hot hydrogen burning

2.3 Hot hydrogen burning beyond the CNO mass region

In the temperature range for hot hydrogen burning (T=0.1-0.4 GK) there is almost no leakage of material from the CNO region to the A>20. Then, hot hydrogen burning can only takes place in massive AGB stars or novae with pre-existing A>20 nuclei. Again the proton capture will compete with β^+ decays.

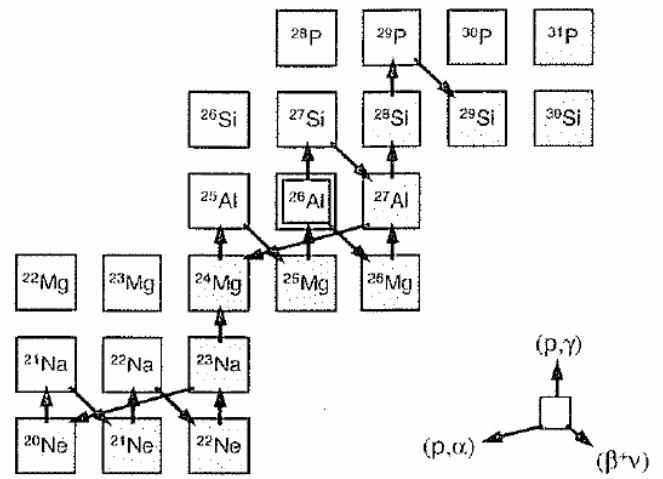

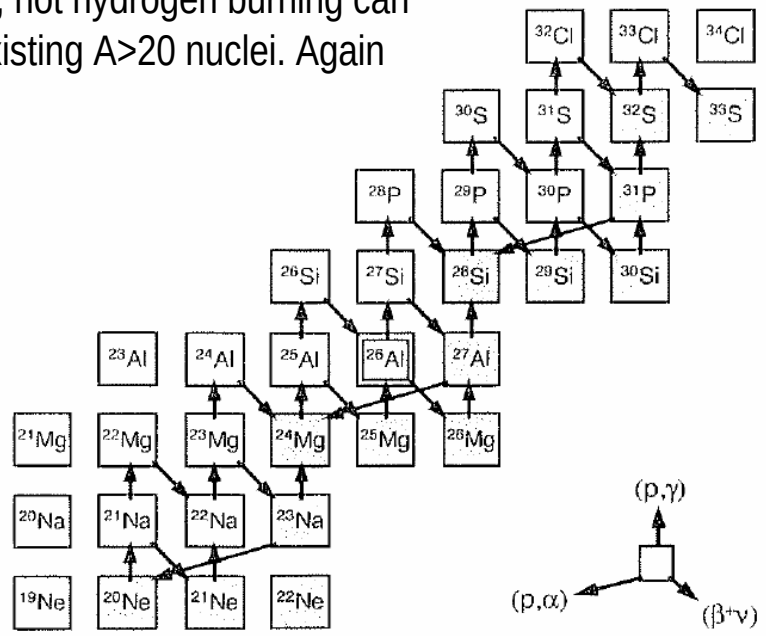

Novae systems with heavier white dwarfs made mainly of O and Ne are good candicates for hot hydrogen processes beyond the CNO mass region. The exact path for nucleosynthesis is very much temperature dependent. In Novae models achieving peak temperatures at 0.25 GK, β^+ decays of ^{23}Mg, ^{25}Al and ^{27}Si are faster than proton-capture reactions and, therefore, nucleosynthesis runs close to the line of stable nuclei.

Hot hydrogen burning

2.4 Experimental investigation

With one exception, none of the reactions involving Unstable target nuclei in the A=20-40 range have been measured directly. Their reaction rates are estimated indirectly from nuclear structure information. Hence, rate errors for reactions such us $^{23}Mg(p,\gamma)^{24}Al$, $^{25}Al(p,\gamma)^{26}Si$ and $^{27}Si(p,\gamma)^{28}P$ may amount to an order of magnitude or more.

The exception is the $^{21}Na(p,\gamma)^{22}Mg$ reaction which influences the production of ^{22}Na in novae. The decay of 22Na(T1/2=2.6 y) produced γ-rays with an energy of 1275 keV. This g-rays may be observed with detectors onboard satellites and be used for investigating classical Novae phenomenon.

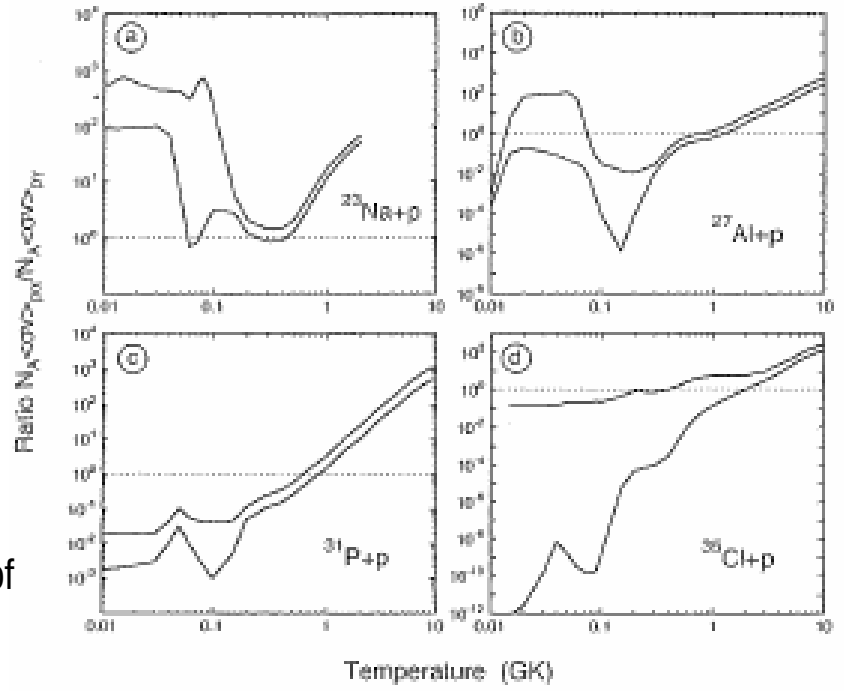

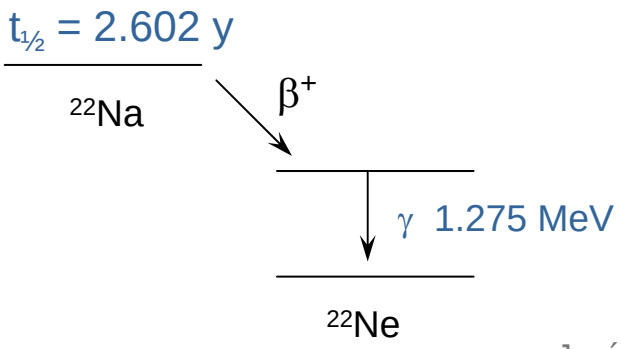

Hot hydrogen burning

2.4 Experimental investigation: example

$^{26}Si(p,\gamma)^{27}P$ and the production of ^{26}Al

This reaction hinderes the production of ^{26}Al but it is difficult to investigate because the two nuclei involved are unsstable.

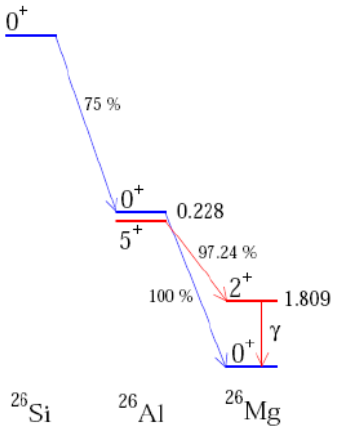

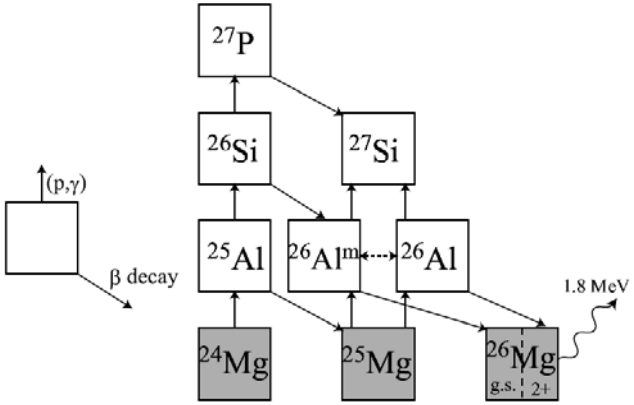

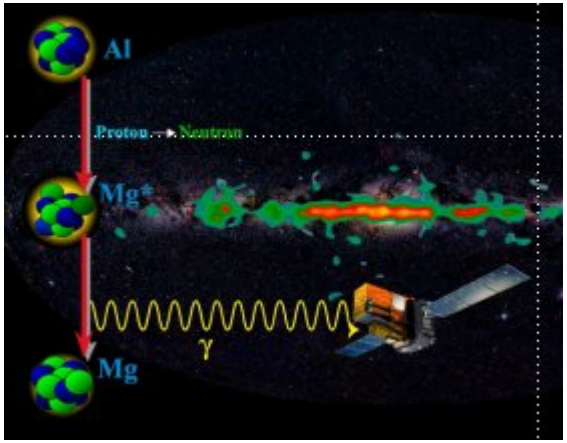

One can uses indirect methods as the reverse Coulomb dissociation reaction $^{27}P(\gamma,p)^{26}Si$, but still ^{27}P must be produced in a previous reaction.

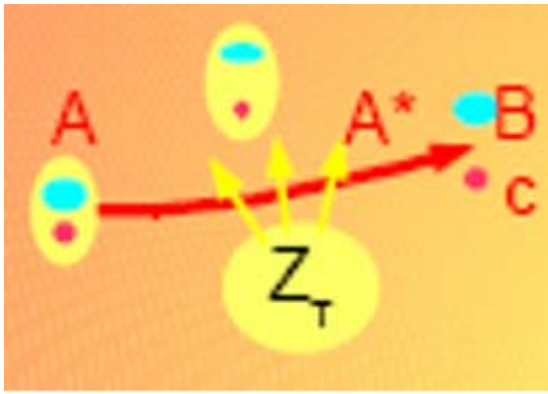

Hot hydrogen burning

2.4 Experimental investigation: e

$^{26}Si(p,\gamma)^{27}P$ and the production of ^{26}A

The experiment was performed at GSI Darm

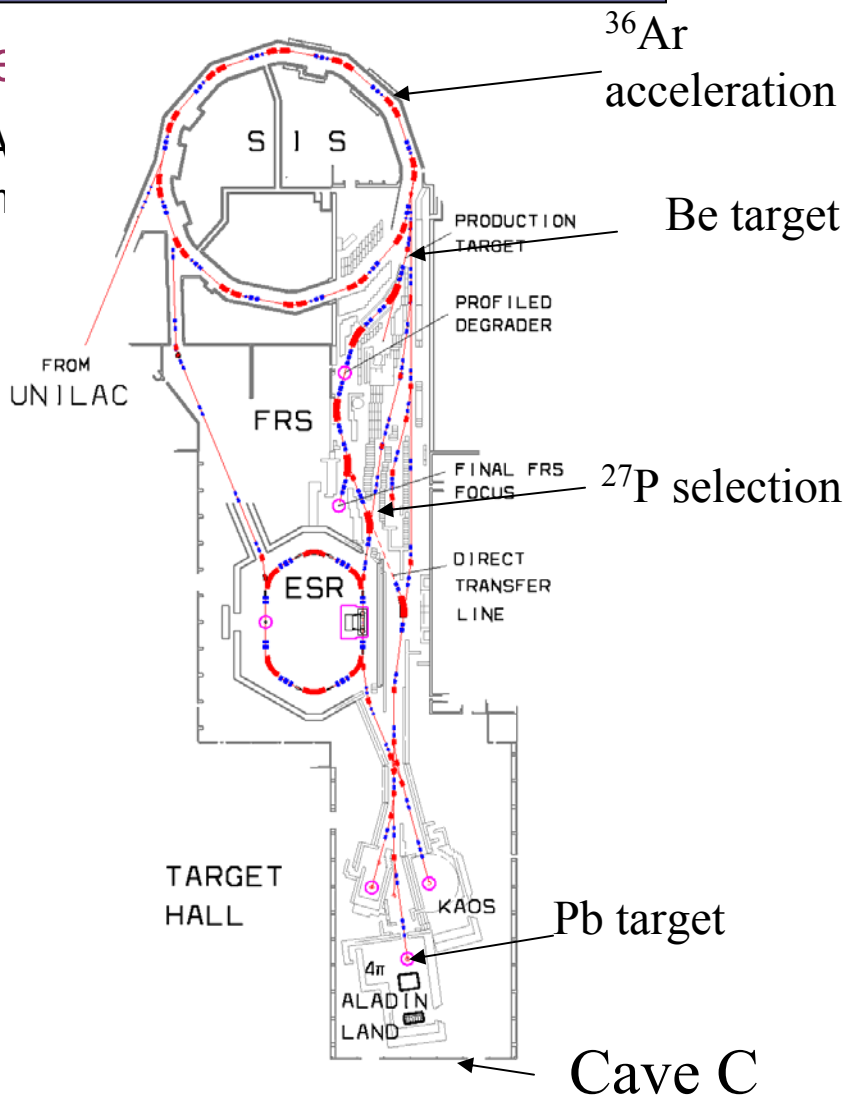

Hot hydrogen burning

2.4 Experimental investigation: example

$^{26}Si(p,\gamma)^{27}P$ and the production of ^{26}Al

Experimental setup

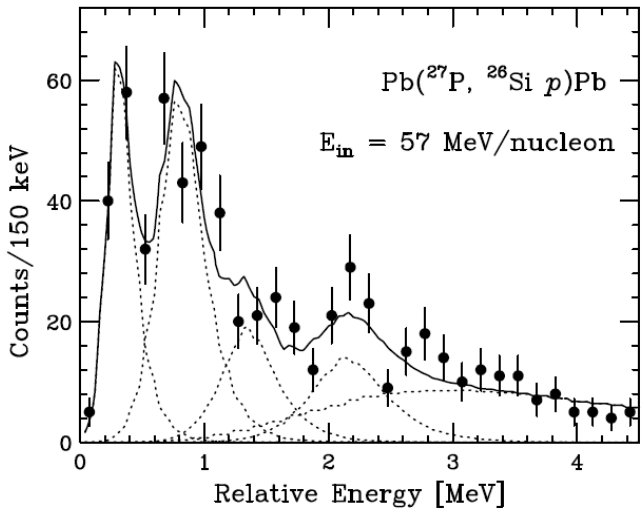

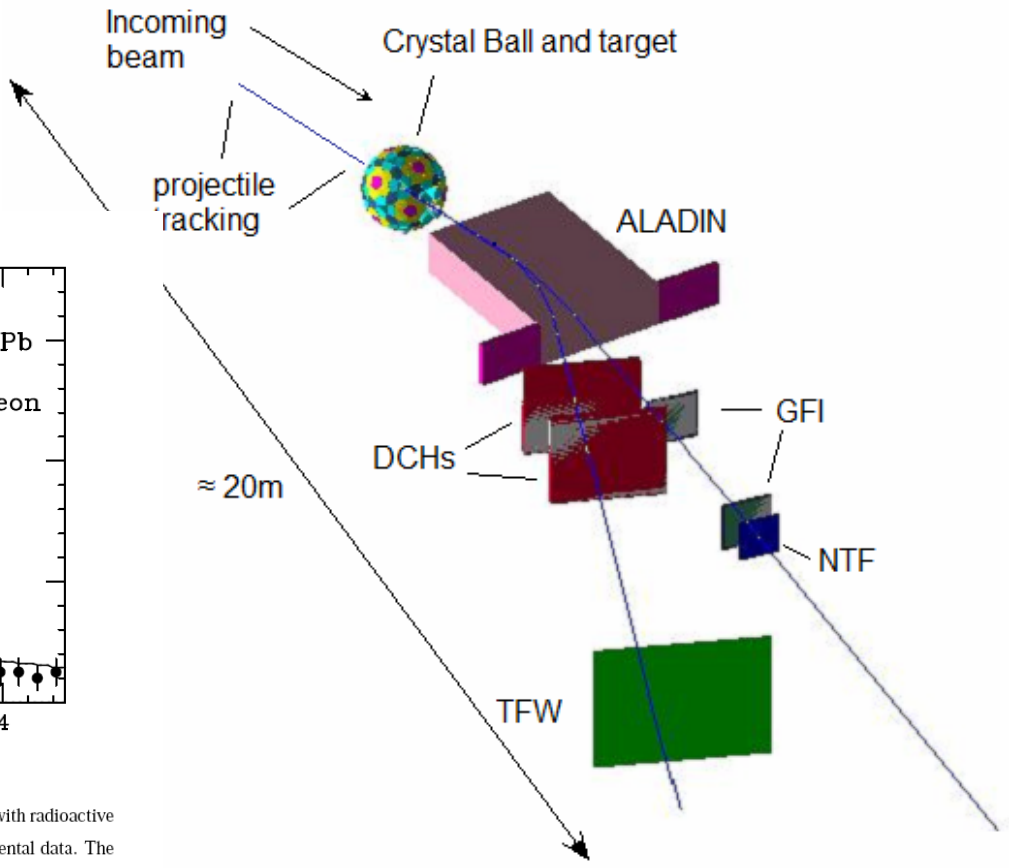

Figure 4.2: Relative energy spectrum of the Pb(^{27}P,^{26}Si p)Pb reaction measured with radioactive ^{27}P beam of 57 MeV/nucleon incident energy. Filled circles shows the experimental data. The solid curve represents the best fit by the five components shown individually by the dotted curves which represent four excited states and a direct capture component.

Hydrostatic helium burning

3.1 Stellar scenario

When a star exhausts the supply of hydrogen by nuclear fusion processes in its core, the core contracts and its temperature increases, causing the outer layers of the star to expand and cool. The star's luminosity increases greatly, and it becomes a red giant, following a track leading into the upper-right hand corner of the HR diagram.

Eventually, once the temperature in the core has reached approximately 0.1–0.4 GK, and density is of the order of 10^2-10^5 g/cm^{-3}, helium burning begins. The onset of helium burning in the core halts the star's cooling and increase in luminosity, and the star instead moves back towards the left hand side of the HR diagram. This is the horizontal branch

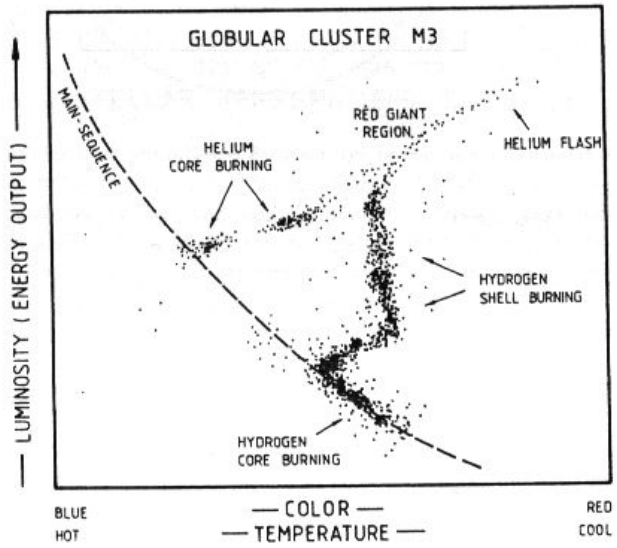

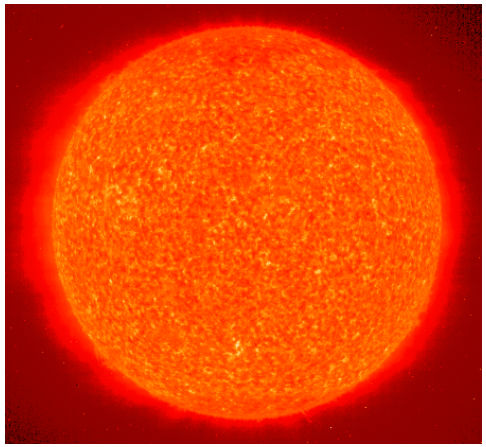

Hydrostatic helium burning

3.2 Helium-burning reactions

The helium burning process leading to the production of ^{12}C and ^{16}O has not been understood for some time. The fact that no stable nucleides with mass numbers A=5 and A=8 exist represented at major hurdle in this regard. Both, the simultaneus and sequential triple-α fusion could not explain the observed ^{12}C and ^{16}O abundances until Hoyle proposed (1954) that the $^{8}B(\alpha,\gamma)^{12}C$ reaction proceeded via an s-wave resonance.

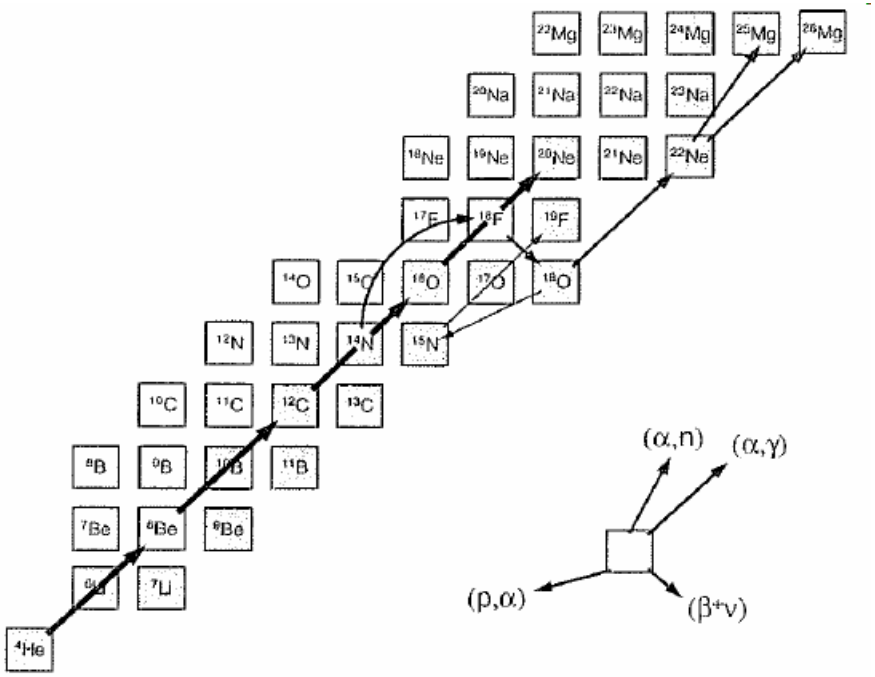

$$^{4}He + ^{4}He \rightarrow ^{8}Be \quad (Q = -0.091\,MeV)$$

$$^{4}He + ^{8}Be \rightarrow ^{12}C \quad (Q = 7.37\,MeV)$$

$$^{4}He + ^{12}C \rightarrow ^{16}O + \gamma$$

$$^{4}He + ^{16}O \rightarrow ^{20}Ne + \gamma$$

$$^{4}He + ^{20}Ne \rightarrow ^{24}Mg + \gamma$$

Hydrostatic helium burning

3.3 3α reaction

According to Hoyle's prediction, the overall conversion of three α-particles into one ^{12}C nucleus during helium burning would be too slow unless the second step proceeds via an s-wave resonance ($J^{\pi}=0^{+}$).

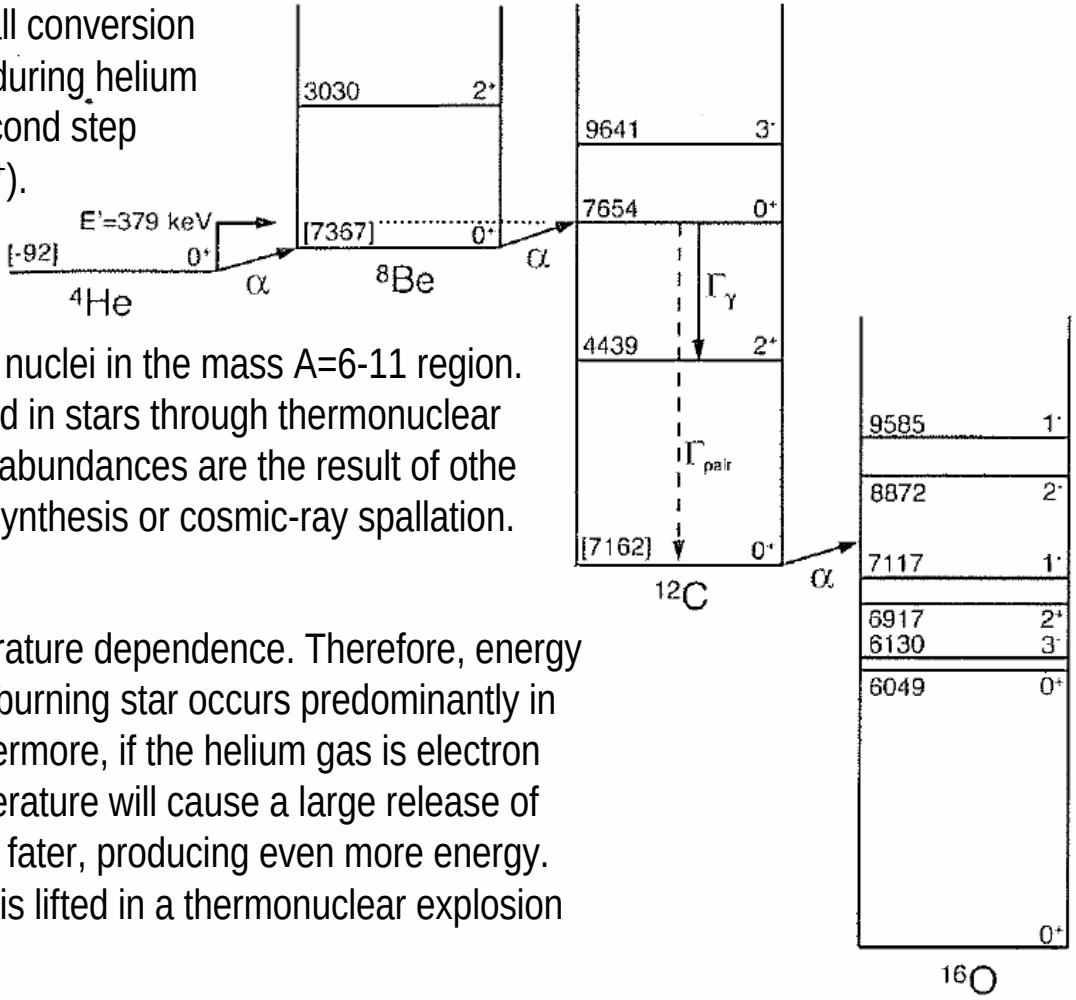

The three α reaction bypasses the stable nuclei in the mass A=6-11 region. Therefore, these nuclei are not synthetized in stars through thermonuclear Reactions. Their extremely low observed abundances are the result of othe Processes, such as the Big Bang nucleosynthesis or cosmic-ray spallation.

The 3α reaction has a remarkable temperature dependence. Therefore, energy generatio via the 3α reaction in a helium-burning star occurs predominantly in the regions of highest temperature. Furthermore, if the helium gas is electron degenerate, then a small rise in the temperature will cause a large release of energy. As a result, the temperature rises fater, producing even more energy. The cycle continues until the degeneracy is lifted in a thermonuclear explosion called *helium flash*.

Hydrostatic helium burning

3.4 Other helium-burning reactions

The fact that the ratio of abundances of ^{12}C and ^{16}O in the Universe amounts to $N(^{12}C)/N(^{16}O)\sim0.4$ Suggests that the $^{12}C(\alpha,\gamma)^{16}O$ reaction is rather slow and that, as a result, some ^{12}C remains after helium is exhausted. Therefore, the precise magnitude of the reaction $^{12}C(\alpha,\gamma)^{16}O$ will have a strong Influence on the relative production of ^{12}C and ^{16}O but also on the production of many other elements up to iron and even in the evolution of massive stars that explode as supernovae.

Similarly, the reaction $^{16}O(\alpha,\gamma)^{20}Ne$ must also be rather slow. Indeed, the production of ^{20}Ne and ^{24}Mg is very small, with final mass fractions of the order of 10^{-6} and 10^{-14}, repectively.

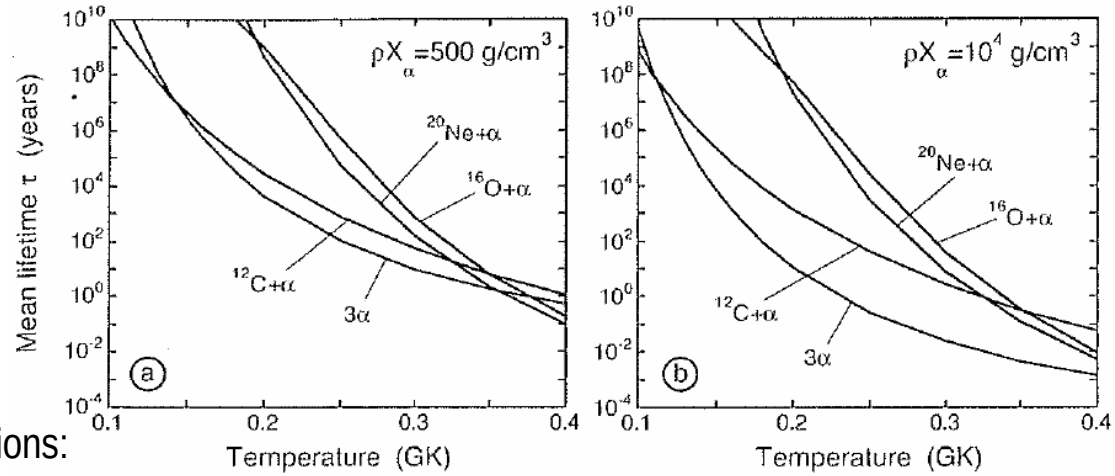

Other helium-burning reactions are due to the presence of ^{14}N as a result of the CNO-cycle operation leading to the reactions:

$$^{14}N(\alpha,\gamma)^{18}F(\beta^{+}\nu)^{18}O(\alpha,\gamma)^{22}Ne$$

Then, ^{22}Ne will be converted in ^{25}Mg and ^{26}Mg by the reactions:

$$^{22}Ne(\alpha,\gamma)^{26}Mg \quad (Q = 10.62\ \mathrm{MeV})$$

$$^{22}Ne(\alpha,n)^{25}Mg \quad (Q = -0.48\ \mathrm{MeV})$$

The latter reaction provides at T>0.25 GK an important source of neutrons that influence sesitively the Synthesis of neutron-rich nuclei in the mass A=60-90 range.

Advanced burning stages

5.1 Stellar scenario

Stars with initial masses exceeding ~11 M_O are capable of igniting successive burning stages in their cores using the ashes of the previous core burning stage as a fuel. Three distinct burning stages follow carbon burning, neon, oxygen and silicon burning. During hydrogen and helium burning, nuclear energy is almost exclusively converted to light. During the advanced burning stages energy is almost enterely radiated as neutrino-anti-neutrino pairs.

After the silicon has been exhausted in the core, the star become an onion-like structure with several layers of different composition separated by thin nuclear burning shells, with the heavier and most stable nuclei in the core composed by electron-degenerate matter.

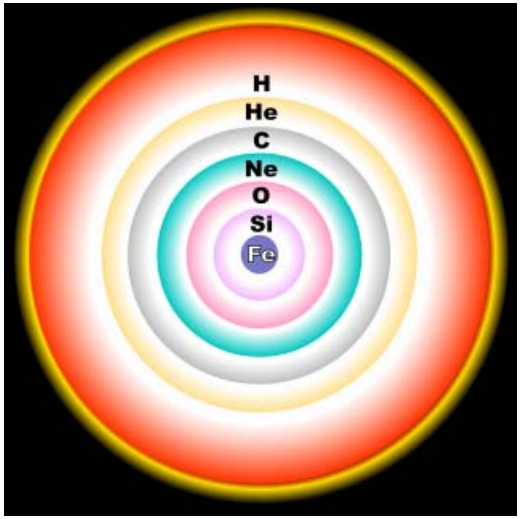

When the mass of the core exceeds the Chandrasekhar limit (~1.4M_O), the electron degeneracy preassure is unable to counteract gravity, and the core collapses photodisintegrating the iron peak nuclei into lighter and less stable elements. When the density reaches values of the order of the nuclear density (~10^{14} g/cm^3), nuclei and nucleons feel the short range nuclear force. Then, the nuclear potential will store energy until it rebounds giving rise to an outward moving shock wave while the very hot and dense inner core becomes a proto-neutron star with a mass of around 1.5 M_O.

Advanced burning stages

5.2 Carbon burning

Massive stars ($8M_O$<M) become red giants during a not degenerate helium burning phase producing an electron-degenerate carbon-oxygen core. Eventually the temperature of the core becomes sufficient for carbon burning, entering the star a *super giant phase* when hydrogen in the outer layers stars burning. Once carbon is exhausted the stellar core is composed mainly by oxygen and neon. If the mass of the star is M<$11M_O$ then it will die as an *oxygen-neon white dwarf*, otherwise the star will continue burning heavier nuclei.

The fusion of two ^{12}C nuclei leads to a highly excited ^{24}Mg (E*>14 MeV). This energy excess is most effectively removed by emission of light particles, being the most important reaction channels:

$$^{12}C(^{12}C, p)^{23}Na \quad (\mathrm{Q} = 2241\,\mathrm{keV})$$
$$^{12}C(^{12}C, \alpha)^{20}Ne \quad (\mathrm{Q} = 4617\,\mathrm{keV})$$
$$^{12}C(^{12}C, n)^{23}Mg \quad (\mathrm{Q} = -2599\,\mathrm{keV})$$

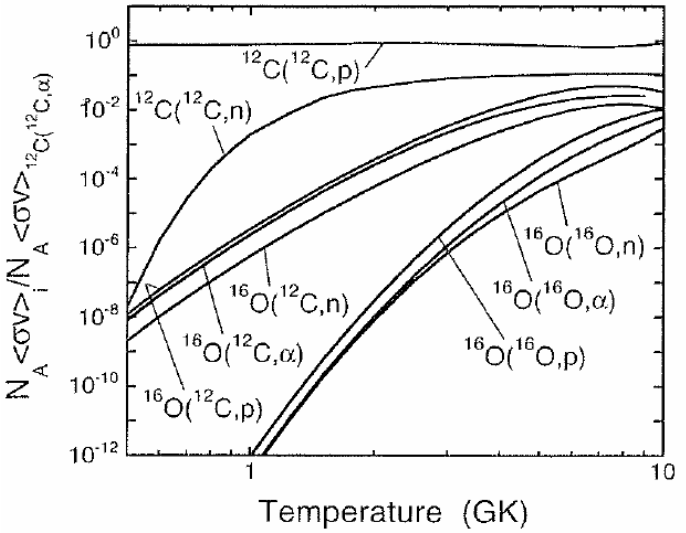

The produced protons, a-particles and neutrons will be quickly consumed at elevated temperatures by initiating Secondary reactions involving the ashes of helium burning (12C and 16O) and the heavy products of the primary Reactions (23Na and 20Ne.) This network of primary and secondary reactions is known as carbon burning. typical temperatures in core carbon burning amount to *T=0.6-1.0 GK* and *T=1.8-2.5 GK* in explosibe burning.

Advanced burning stages

5.2 Carbon burning

The main nuclei involved in the carbon burning and their abundance evolution is shown in the figures. The dominant abundace flows are due to the primary reactions $^{12}C(^{12}C,p)^{23}Na$ and $^{12}C(^{12}C,\alpha)^{20}Ne$ and the reactions induced by the liberated protons and a-particles $^{23}Na(p,\alpha)^{20}Ne$ and $^{16}O(\alpha,\gamma)^{20}Ne$.

Weaker but substantial flows are due to the (p,γ) reactions on ^{21}Ne, ^{22}Ne, ^{23}Na, ^{25}Mg and ^{26}Mg, the (α,γ) reaction on ^{20}Ne, the (α,n) reactions on ^{13}C, ^{21}Ne, and ^{22}Ne, the (n,p) reaction on ^{22}Na and the β^+-decay of $^{26}Al^m$.

(α,n) reactions are of particular interest because they constitute the possible neutron sources playing an important role in the nucleosynthesis above A>60.

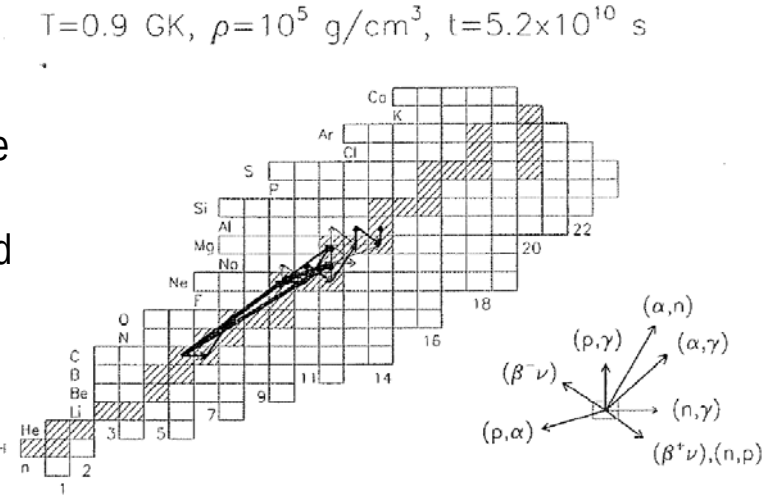

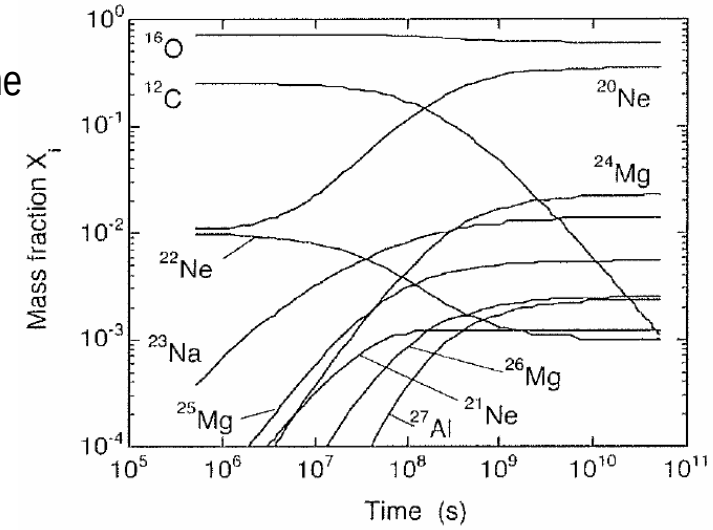

Advanced burning stages

5.3 Neon burning

At the end of the carbon burning, the stellar core consists mainly of ^{16}O, ^{20}Ne, ^{23}Na and ^{24}Mg. When most of the ^{12}C is consumed, the core contracts gravitationally and temperature and density increase until new reactions ignite. Contrary to expectation, the next nuclear fuel to ignite is not oxygen via the $^{16}O+^{16}O$ fusion reaction, but neon burning in α–particle induced reactions. The reason is that after carbon burning the core temperatures Are high enough (*T>1GK*) to initiate photodisintegration reactions, particularly of ^{20}Ne because this is the component of the stellar core with the lowest α-particle separation energy. The liberated α-particles, in turn, induce secondary reactions involving any of the more abundant nuclei.

Primary reaction:

$^{20}Ne(\gamma,\alpha)^{16}O$ (Q=-4730 keV)

Secondary reactions:

$^{20}Ne(\alpha,\gamma)^{24}Mg(\alpha,\gamma)^{28}Si$ (Q=19300 keV)

$^{23}Na(\alpha,p)^{26}Mg(\alpha,n)^{29}Si$ (Q=1855 keV)

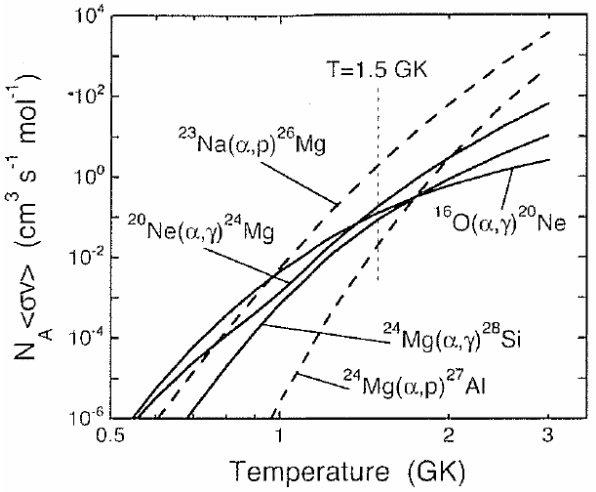

Although the primary reaction is endothermic, the combination with the subsequent secondary reactions leads to a net production of energy as a consequence of the photodisintegration of ^{20}Ne.

Typical temperatures during core neon burning are in the range T=1.2-1.8 GK and in explosive burning stages in the range T=2.5-3.0 GK.

Advanced burning stages

5.3 Neon burning

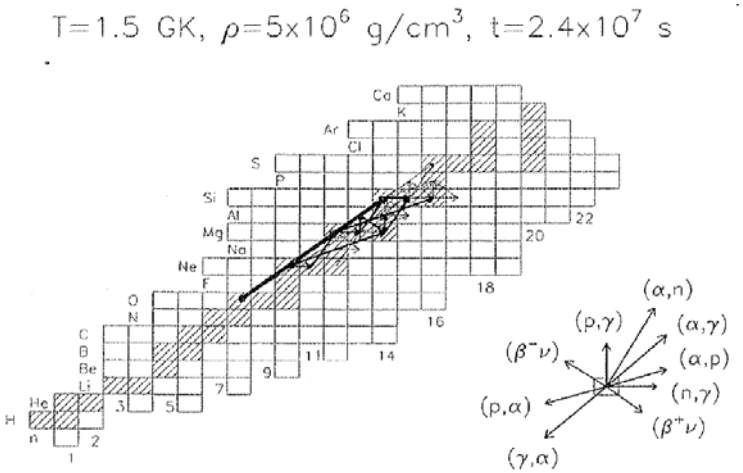

The main nuclei involved in the neon burning and their abundance evolution is shown in the figures. The dominant abundace flows are due to the reactions $^{20}Ne(\gamma,\alpha)^{16}O$ and $^{20}Ne(\alpha,\gamma)^{24}Mg(\alpha,\gamma)^{28}Si$. Smaller but substantial flows are caused by $^{24}Mg(\alpha,p)^{27}Al(\alpha,p)^{30}Si$ and $^{23}Na(\alpha,p)^{26}Mg$.

The released protons initiate a number of (p,γ) reactions on ^{26}Mg, ^{23}Na and ^{25}Mg. Neutrons are also produced in (α,n) reactions on ^{21}Ne, ^{25}Mg and ^{26}Mg.

The 20Ne fuel is exhausted after 280 d being the most abundant nuclei produce in this process ^{16}O, ^{24}Mg and ^{28}Si.

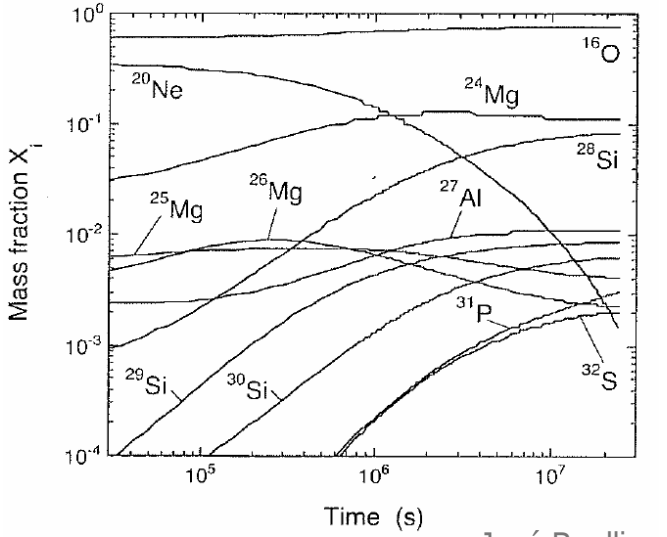

Advanced burning stages

5.4 Oxygen burning

After the neon fuel has been consumed, the most abundant nuclei in the stellar core are ^{16}O, ^{24}Mg and ^{28}Si. If the mass of the star is $M>15M_O$ (super red-giant) the core contracts gravitationally, temperature and density increase and oxygen burning via $^{16}O+^{16}O$ fusion reactions start. Also in this case, the ^{32}S nuclei produced in the fusion reactions are highly excited and they de-excite by emitting several particles and defining the oxygen burning process

$^{16}O(^{16}O,p)^{31}P$	(Q=7678 keV)
$^{16}O(^{16}O,2p)^{30}Si$	(Q=381 keV)
$^{16}O(^{16}O,\alpha)^{28}Si$	(Q=9594 keV)
$^{16}O(^{16}O,2\alpha)^{24}Mg$	(Q=-390 keV)
$^{16}O(^{16}O,d)^{30}P$	(Q=-2409 keV)
$^{16}O(^{16}O,n)^{31}S$	(Q=1499 keV)

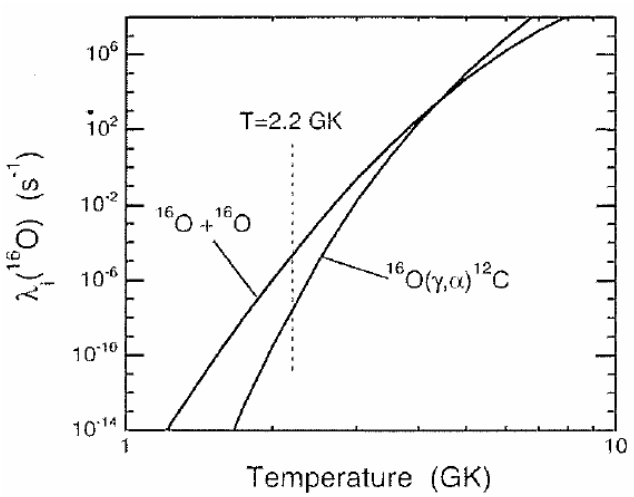

The liberated light particles are quickly consumed by secondary reactions involving the ashes of neon burning or heavy nuclei produced in the fusion of $^{16}O+^{16}O$. Typical temperatures during core oxygen burning are in the range T=1.5-2.7 GK. In explosive oxygen burning, temperatures of T=3-4 GK are reached.

Advanced burning stages

5.4 Oxygen burning

Many different nuclear processes occur during oxygen burning. The largest net abundance flows correspond to the primary $^{16}O+^{16}O$ reaction producing ^{28}Si and ^{32}S via the following reactions:

$^{16}O(^{16}O,p)^{31}P(p,\gamma)^{32}S$

$^{16}O(^{16}O,p)^{31}P(p,\alpha)^{28}Si$

$^{16}O(^{16}O,\alpha)^{28}Si$

$^{16}O(^{16}O,n)^{31}S(\gamma,p)^{30}P(\gamma,p)^{29}Si(\alpha,n)^{32}S$

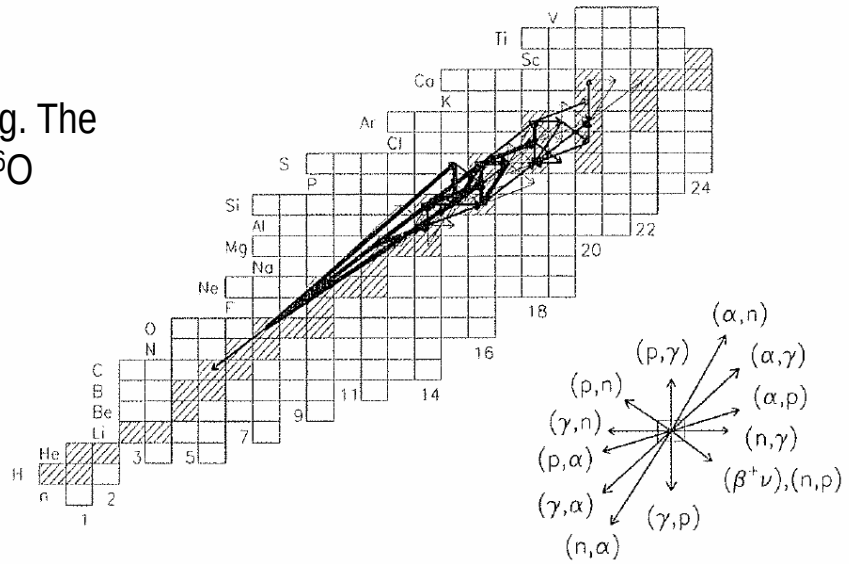

Then, some of the ^{28}Si nuclei are converted to ^{32}S via $^{28}Si(\alpha,\gamma)^{32}S$. A fraction of the ^{32}S in either transformed back to ^{31}P via $^{32}S(n,\gamma)^{33}Sn(n,\alpha)^{30}Si(p,\gamma)^{31}P$ or is converted to heavier nuclei via $^{32}S(\alpha,p)^{35}Cl(p,\gamma)^{36}Ar$.

^{16}O, $^{24,25,26}Mg$ and ^{27}Al nuclei are quickly depleted with progressing time. The ^{16}O fuel is exhausted after about 162 days. The most abundant nuclei at the end are: ^{28}Si (X_f=0.54), ^{32}S(X_f=0.28), ^{38}Ar(X_f=0.084), ^{34}S(X_f=0.044), ^{36}Ar(X_f=0.027) and ^{40}Ca(X_f=0.021).

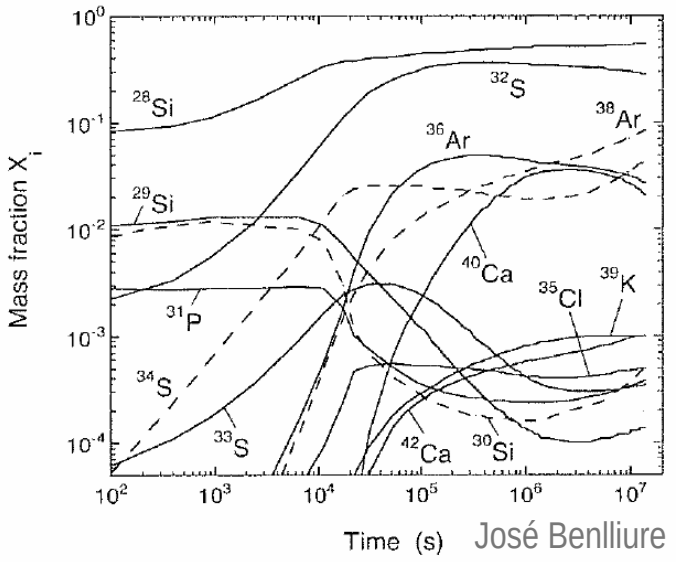

Advanced burning stages

5.5 Silicon burning

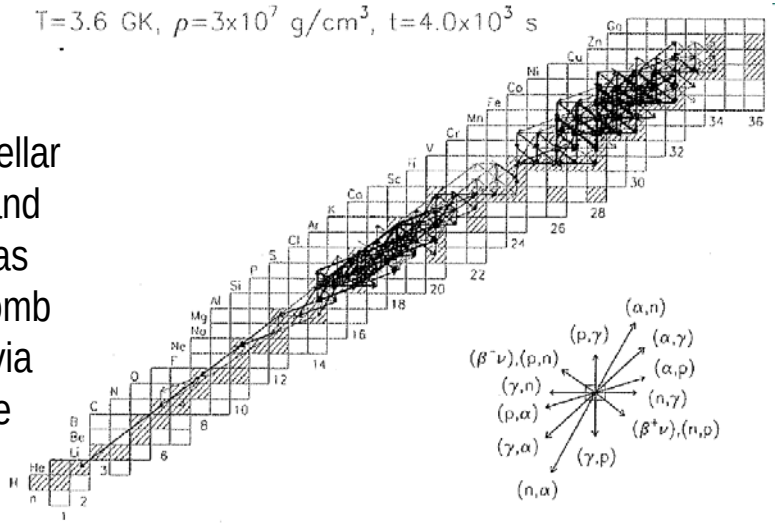

Near the conclusion of core oxygen burning, when the ^{16}O fuel is depleted, the most abundant nuclei are ^{28}Si and ^{32}S. If the stellar mass in $M>M_O$ (pre-supernova star) the stellar core contracts and the temperature and density increases. Fusion reactions such as $^{28}Si+^{28}Si$ or $^{28}Si+^{32}S$ are too unlikely to occur because of Coulomb barrier considerations. Instead, the nucleosynthesis proceeds via photodisintegrations of less tightly bound nuclei and the capture of the liberated light particles to create gradually heavier and more tightly bound nuclei.

Temperatures during core silicon burning are in the range of T=2.8-4.1 GK, depending on the stellar mass. Explosive silicon burning takes place in the range of 4-5 GK.

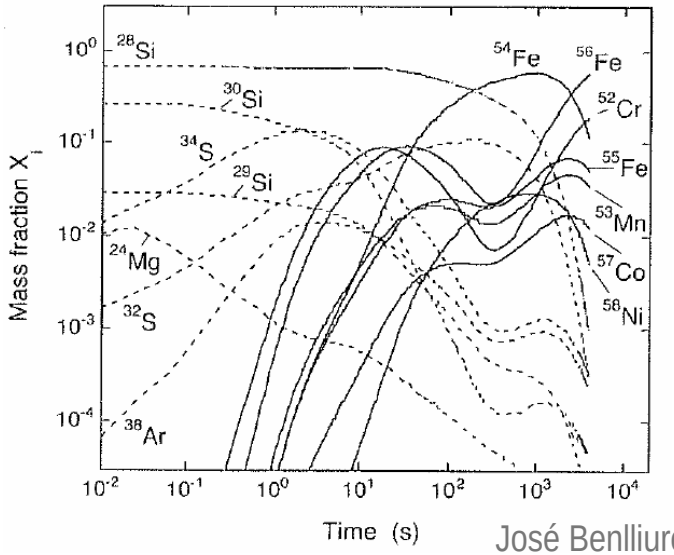

Stelar nucleosynthesis of light nuclei (A<60)

Exercise 1.
Determine the average time to observe a single p(p,$e^+\nu$)d reaction in an experiment using a proton accelerator with an intensity of 1 A and an energy of 1 MeV, and a hydrogen target with a density of 10^{20} protons/cm^2. For the cross section consider that the corresponding S-factor is described by the following expression.

$$S(E) = 3.94 \cdot 10^{-25} + 4.61 \cdot 10^{-24} E + 2.96 \cdot 10^{-23} E^2$$

Exercise 2.
Calculate